Available online at www.sciencedirect.com
SCIENCE DIRECT
Journal of Power Sources 158 (2006) 428–435
JOURNAL OF POWER SOURCES
www.elsevier.com/locate/jpowsour

System modeling of an air-independent solid oxide fuel cell system for unmanned undersea vehicles

A. Alan Burke *, Louis G. Carreiro

Naval Undersea Warfare Center, Division Newport, 1176 Howell Street, Bldg. 1302/2, Newport, RI 02841, USA

Received 19 August 2005; accepted 16 September 2005
Available online 14 November 2005

Abstract

To examine the feasibility of a solid oxide fuel cell (SOFC)-powered unmanned undersea vehicle (UUV), a system level analysis is presented that projects a possible integration of the SOFC stack, fuel steam reformer, fuel/oxidant storage and balance of plant components into a 21-in. diameter UUV platform. Heavy hydrocarbon fuel (dodecane) and liquid oxygen (LOX) are chosen as the preferred reactants. A maximum efficiency of 45% based on the lower heating value of dodecane was calculated for a system that provides 2.5 kW for 40 h. Heat sources and sinks have been coupled to show viable means of thermal management. The critical design issues involve proper recycling of exhaust steam from the fuel cell back into the reformer and effective use of the SOFC stack radiant heat for steam reformation of the hydrocarbon fuel.
Published by Elsevier B.V.

Keywords: Unmanned underwater vehicle; Unmanned undersea vehicle; Thermal management; Air-independent fuel cell

1. Introduction

The US Navy's intended use of unmanned undersea vehicles (UUVs) for surveillance and reconnaissance in the littoral environment requires the development of high-energy power sources that can support long duration missions. Unlike their torpedo counterparts, UUVs value stealth and endurance over power and speed. A strong effort has been made to increase UUV mission duration and design a UUV platform that offers modularity in a 21″ hull, which enables deployment from torpedo tubes in submarines.

While batteries are typically employed to power UUVs, they lack sufficient energy density to carry out extended missions. One alternative to batteries is the solid oxide fuel cell (SOFC), which offers the advantages of easy refueling and high efficiency operation with logistic-type fuels such as JP-8. Combustion engines also offer ease of refueling and quick turn around time, but this is at the expense of low overall system fuel efficiency (∼15–25%) and a significant noise signature. Semi-fuel cells have been studied as well, but these cells consume the metallic anode, so the entire energy system needs to be replaced after each run [1]. In contrast, the solid oxide fuel cell is a low-noise, highly efficient, solid state device that can operate using reformed logistics fuels. Unlike proton exchange membrane fuel cells (PEMFC) or alkaline fuel cells, SOFCs can tolerate carbon monoxide and low concentrations of sulfur (<100 ppm), which are by-products of reformed logistics fuel [2]. In addition, SOFCs have shown efficiencies over 50% LHV_{fuel} [3,4] and fuel versatility better than all other fuel cells [5].

The 21″ UUV will require a maximum continuous net power output of 2.5 kW for its mission lifetime. The targeted energy density and specific energy of the entire energy section are 500 W h L^{-1} and 450 W h kg^{-1}, respectively, whereas the minimum acceptable values would be 360 W h L^{-1} and 330 W h kg^{-1} [6]. Fig. 1 shows the overall process diagram for the energy section modeled in this study. Table 1 gives specific stream data used in thermodynamic calculations. Preliminary analysis has been done at ambient pressure.

The main motor for UUV propulsion requires a 70–80 V main buss with 28 V for vehicle systems and sensors. The UUV draws approximately 17 A when moving at 4 knots at a power level of 1300 W. The maximum continuous load is 2500 W (28 A), at which the UUV reaches 7 knots. The targeted lifetime of each mission is greater than 40 h, and the vehicle sortie reach is greater

* Corresponding author. Tel.: +1 401 832 6675; fax: +1 401 832 2908.
E-mail addresses: burkeaa@npt.nuwc.navy.mil, carreirolg@npt.nuwc.navy.mil (A.A. Burke).

0378-7753/$ – see front matter. Published by Elsevier B.V.
doi:10.1016/j.jpowsour.2005.09.042

Nomenclature

A_s	surface area of SOFC stack(s) (m^2)
$C_{p,i}$	heat capacity of species i ($J\,mol^{-1}$)
d	gap thickness between SOFC stack and enclosure (m)
f_{12}	view factor of gray surfaces (stack surface to, enclosure surface)
h	convective heat transfer coefficient from stack surface ($W\,m^{-2}\,K^{-1}$)
I	fuel cell current (A)
k	thermal conductivity ($W\,m^{-2}\,K^{-1}$)
$K_{eq,i}$	equilibrium constant for reaction i
n_i	moles of species i (mol)
N	total number of cells in fuel cell stack(s)
Np_r	Prandtl number
N_{Gr}	Grashof number
N_{Nu}	Nusselt number
Q_i	heat loss from/generation by i (W)
s	constant (5.676 e-8 $W\,m^{-2}\,K^{-4}$)
T	temperature (K)
$V_{operating}$	operational voltage (V)
V_{th}	thermal neutral voltage (V)
x	number of moles of hydrogen formed in shift reaction (mol)
?	efficiency (%)
$?_{rxn}H_i$	heat of reaction for species i ($J\,mol^{-1}$)
$?_{Vap}H_i$	heat of vaporization for species i ($J\,mol^{-1}$)

than 75 nautical miles. Total energy requirement is estimated at 100 kW-h, which is based on 2500 W for 40 h.

2. System design issues for sofc energy section

2.1. SOFC stack design

An anode-supported SOFC is the basis for this design model. The thin electrolyte (~5–10 μm) enables the cells to minimize ohmic resistance and operate at 750–850 °C (1023–1123 K). Operation in this temperature range allows the interconnect materials to be metallic, which would have lower resistance and higher thermal conductance than ceramic interconnects. This would also reduce the cost of the interconnect materials and lower the operating temperatures of ancillary equipment, such as the reformer, burner, and heat exchangers. The lower temperature reduces the thermal stresses on the equipment caused by thermal cycling and creates a larger safety window for potential hot spots in the system.

The active area of each cell is sized at 8 cm × 8 cm, and the addition of cell supports and gas manifolds increase the actual size of each cell to roughly 10 cm × 10 cm. The thickness of each cell will vary according to the interconnect thickness. Assume here that there are three cells per centimeter in thickness. For a 2.5 kW stack in which each cell operates at 0.8 V and 12.8 A, the total number of cells needed is 2500 W/12.8A/0.8 V = 245 cells. Considering that there will be parasitic devices such as system controls, the total cells needed are estimated to be 300. This would require a volume of (300 cells) (0.33 cm $cell^{-1}$(100 cm^2) (10^{-3} L cm^{-3})~10 L.

2.2. Volumetric and mass limitations

Strict limitations are placed on the total volume and mass of the UUV energy section, which includes the fuel cell stack, fuel, oxidizer, reformer, and all other balance of plant components. The 21″ UUV energy section has useable cylindrical dimensions of 43 in. in length and 18.5 in. in diameter. The volume restraint given is based on having a 1.25-in. thick outer hull volume that has been subtracted from the total volume of the energy section. The total available volume is then 189 L (6.67 ft^3) with the mass limit set at 209 kg (462 lb) in order to maintain proper vehicle buoyancy.

2.3. Choice of hydrocarbon fuel

JP-8 is the Navy's ideal fuel of choice, but it is a very complex mixture of heavy hydrocarbons that may contain sulfur concentrations up to 3500 ppm [7,8]. This sulfur can degrade catalyst and fuel cell components over time. For the purposes of this study, dodecane has been modeled as a sulfur-free surrogate fuel for JP-8. It has similar energy density, high flash point, and it can tolerate lower steam-to-carbon ratios in the reforming process. Low-sulfur diesel fuel is another option that will keep fuel price low, but the advantage of using a clean, specialty fuel like dodecane to preserve system component lifetimes could outweigh its higher fuel price in the modestly sized UUV marketplace.

2.4. Fuel reforming

An essential component of this system is the reformer. Steam reforming (SR) was selected over catalytic partial oxidation and autothermal reforming because it offers the highest theoretical efficiency by producing more moles of hydrogen per mole of fuel consumed. SR will ensure a richer fuel stream into the SOFC stack as lon&as the steam-to-carbon ratio is kept low (<3.5). Unfortunately, steam reformation (reaction (1)) is very endothermic and requires excessive heat to sustain the reaction. This heat can be supplied by three sources: a burner coupled with a high surface area heat exchanger, the fuel exhaust from the fuel cell, and the radiation/convection from the SOFC stack surfaces. Previous work has shown that a steam-to-carbon ratio of 3.0–3.5 is feasible for steam reforming ideal hydrocarbons while still mitigating carbon deposition [9].

$$C_mH_n + mH_2O + \text{HEAT} \rightarrow \{m + n/2)H_2 + mCO \quad (1)$$

Regardless of the type of reformer chosen, high system efficiency involves proper thermal management and steam recirculation from the fuel cell into the reforming process. Recovering hydrogen from steam via reformation and the water–gas shift reaction, reaction (2), is a vital part of maintaining high hydrogen

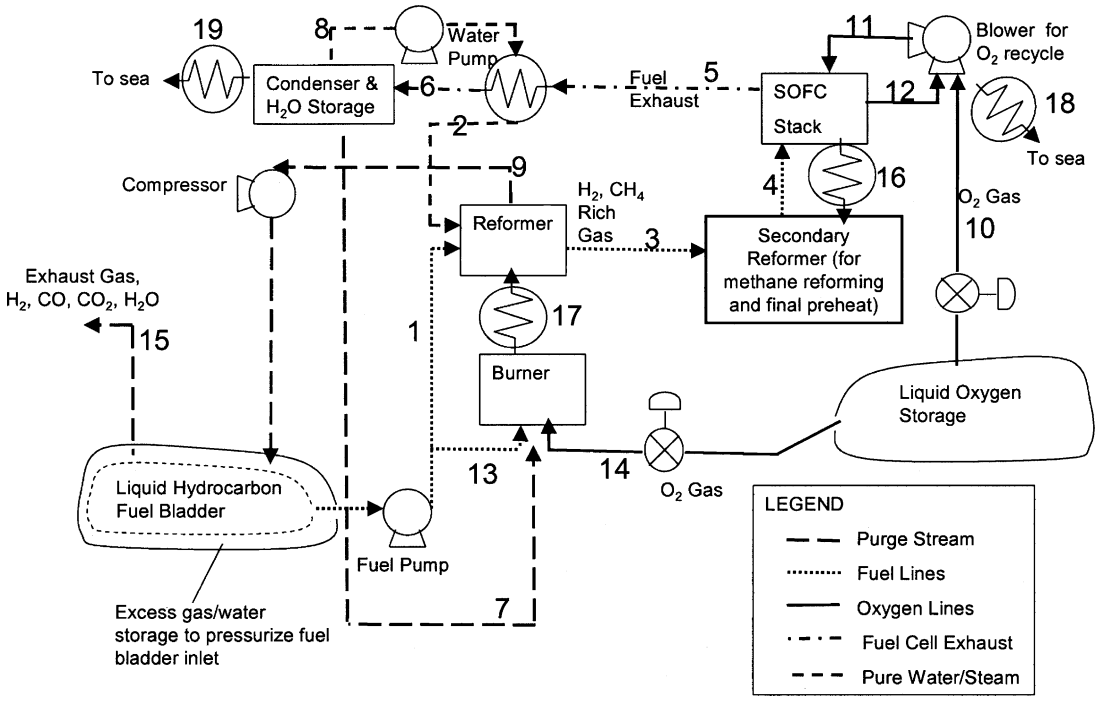

Fig. 1. Process flow diagram of SOFC power system.

concentration for the fuel feed. The high steam content (~30% inlet) of the fuel stream also helps to prevent carbon deposition and provide more thermal mass for cooling the stack. The high hydrogen concentration (~50% at the inlet) aids in minimizing concentration polarization in the fuel cell as ~75% fuel utilization is obtained. Button cell tests have shown that at the current densities anticipated (0.10–0.30 A cm^{-2}), concentration polarization only becomes severe below 10% H_2.

$$H_2O + CO \rightarrow H_2 + CO_2 \quad (2)$$

2.5. Steam recycling

Three different steam-recycling schemes were considered. In the first approach, pure steam is recycled from the fuel cell product gas back into the steam reformer, which generates a fresh feed of hydrogen-rich gas for the fuel cell. In this case, a condenser is used to separate water from other fuel cell products, and a heat exchanger is used to regenerate steam from this collected water. Another option is to split the fuel cell product gas stream and divert part of it directly into the reformer. This eliminates the

Table 1
Thermodynamic table for Fig. 1, stream attributes

Stream	T (K)	P (psi)	Composition (%)						Flow (mol min^{-1})	Enthalpy (h-h298) (J mol^{-1})	Q (W)
			H_2	CO	CO_2	H_2O	$C_{12}H_{26}$	O_2			
1	298	14.7	0.00	0.00	0.00	0.00	1.00	0.00	0.042	0	0
2	1110	14.7	0.00	0.00	0.00	1.00	0.00	0.00	1.514	30190	0
3	Under investigation										0
4	1055	14.7	0.49	0.12	0.08	0.32	0.00	0.00	2.564	25850	0
5	1130	14.7	0.11	0.03	0.16	0.70	0.00	0.00	2.564	31840	0
6	373	14.7	0.11	0.03	0.16	0.70	0.00	0.00	2.564	2551	0
7	373	14.7	0.35	0.11	0.54	0.00	0.00	0.00	0.779	2589	0
8	373	14.7	0.00	0.00	0.00	1.00	0.00	0.00	1.514	2535	0
9	1100	14.7	0.12	0.11	0.54	0.23	0.00	0.00	0.779	33500	0
10	298	14.7	0.00	0.00	0.00	0.00	0.00	1.00	0.597	0	0
11	1040	14.7	0.00	0.00	0.00	0.00	0.00	1.00	11.208	24100	0
12	1130	14.7	0.00	0.00	0.00	0.00	0.00	1.00	10.611	27265	0
13	298	14.7	0.00	0.00	0.00	0.00	1.00	0.00	0.000	0	0
14	298	14.7	0.00	0.00	0.00	0.00	0.00	1.00	0.089	0	0
15	298	14.7	0.11	0.08	0.78	0.03	0.00	0.00	0.537	0	0
16											817
17											715
18											320
19											587

need for a heat exchanger/condenser, but fuel dilution and higher pressure will result, raising the concerns of carbon deposition and decreased fuel cell performance. The third option considers the split stream with a high temperature CO_2 scrubber that would help prevent fuel dilution by removing CO_2. Minimizing system volume/mass and maximizing fuel cell performance are the main criteria for selection. For the purpose of this study, the first scheme was chosen to avoid modeling carbon deposition, higher pressure, and CO_2 scrubbing (which has not yet been tailored for this system).

2.6. Oxidant storage

With air not available in the underwater environment, oxygen must be stored onboard the UUV. Molar density and specific mass of each storage method is shown in Table 2. While the solid chemical storage, or lithium perchlorate ($LiClO_4$) candle, has the most efficient storage on a volume basis, the controlled release of oxygen is problematic and has yet to be perfected. Sixty-weight percent hydrogen peroxide (H_2O_2) solution has the least efficient storage, but offers the advantage of producing water, which may be used in the reforming process or as a coolant for the stack. At first glance this seems attractive, however if the system is properly designed the fuel cell should produce more than enough water to be used in the reformer. Hence, the extra storage space required for hydrogen peroxide makes it less viable. Compressed O_2 would be easy to store and control the flow, but the pressure is limited to 3500 psi, as mandated by submarine safety requirements. Liquid oxygen (LOX) offers a much higher volumetric oxygen density, and it does not have the safety issues inherent with high pressure gas storage while the system is not in use. Therefore, LOX has been selected as the method of oxygen storage for this study. However, the values in Table 2 do not account for the storage tanks needed to hold the oxygen source. The cryogenic dewar needed to store LOX will be rather large, heavy, and contribute its own set of safety hazards. For instance, the LOX tank must be cooled and vented as needed to prevent temperature rise within the dewar.

2.7. Oxidant conservation

Commercial SOFC stacks on the kilowatt scale are highly exothermic and require air flows roughly 10 times that of stoichiometric in order to cool the stack. Since a UUV does not have access to a fresh air supply, circulation of oxidant needs to be used to regulate the stack operating temperature. In this system design, the fan or blower must operate at elevated temperature. To tolerate a pure O_2 atmosphere at elevated temperatures, the fan must then be fabricated from materials such as inconel alloy, silica nitride, or high-temperature ceramic. Cooling of the oxidant stream via heat exchange at the hull is indicated by Stream 18 in Table 1.

Table 2
Comparison of oxygen storage methods

Oxygen storage method	Moles O_2 L^{-1}	Moles O_2 kg^{-1}
Liquid oxygen (LOX)	35.6	31.2
Compressed O_2 gas (3500 psig)	9.6	31.2
Hydrogen peroxide @ 40 °C	10.9	8.8
Lithium perchlorate	45.5	18.7

2.8. Thermal management

A maximum UUV chamber temperature of 50 °C (323 K) must be maintained to protect the electronics on board, and heat must be able to dissipate through the UUV hull. Fans inside the UUV will circulate air to aid convection at the hull surface. The efficiency of heat transfer through the hull will depend on the seawater temperature, hull design, and speed of the UUV. At higher speeds, the UUV will be able to dissipate heat faster by maintaining a greater temperature gradient across the hull. This is advantageous, since the UUV generates more heat at higher power levels.

However, there are limitations to cooling through the UUV hull, and this system will be generating considerable heat during operation. It is essential to couple heat sources and sinks to minimize the required heat transfer at the UUV hull, the inner chamber temperature, and the steam reformer burner requirements. Sound thermal management begins with analyzing the SOFC stack and reformer thermal balances. While the gases flowing through the SOFC will aid in cooling the stack, a significant portion of the heat generated by the stack must be emitted by convection and radiation from the surfaces of the stack. This heat dissipation from the SOFC stack surfaces is dependent on the current density, stack/cell size, interconnect material, and enclosure temperature [10,11].

Numerical models of the fuel cell have shown that most of the heat must be removed from the cathode side, as the electrochemical oxidation of H_2 at the anode is slightly endothermic and may produce a temperature gradient across the cell itself [12]. The use of metallic interconnects and anode-supported cells should help limit this effect by keeping thermal conductivity high throughout the stack.

3. Calculations

3.1. SOFC stack thermal balance

In order for the stack to run with a constant temperature profile, the heat generated must equal the heat removed from the stack. The sources of generation are the water–gas shift reaction along with the resistances and polarizations within the stack. These must equal the heat removed by the mass flow of oxidant and fuel gas through the stack combined with the radiant and convective losses from the stack surfaces. Overall, the equation for this SOFC stack operating at steady state is

$$Q_{\text{Stack}} + Q_{\text{Shift,rxn}} + Q_{\text{FuelGas}} + Q_{\text{Oxidant}} + Q_{\text{Radiation}} + Q_{\text{Convection}} = 0 \quad (3)$$

where

$$Q_{\text{Stack}} = (I)(N)(V_{\text{th,cell}} - V_{\text{operating,cell}}) \quad (4)$$

$$K_{\mathrm{eq,Shift},T_{\mathrm{out}}} = \frac{(n_{\mathrm{H_2}} + x)(n_{\mathrm{CO_2}} + x)}{(n_{\mathrm{H_2O}} - x)(n_{\mathrm{CO}} - x)} \quad (5)$$

$$Q_{\mathrm{Shift,rxn}} = \Delta_{\mathrm{rxn}} H_{\mathrm{Shift},298\,\mathrm{K}}(\Delta \dot{n}_{\mathrm{H_2}}) = \Delta_{\mathrm{rxn}} \mathrm{H}_{\mathrm{Shift},298\,\mathrm{K}}(x) \quad (6)$$

$$Q_{\mathrm{FuelGas}} = \sum_{\mathrm{i}} n_{i,\mathrm{out}} \int_{298}^{\mathrm{Tout}} C_{p,i}\mathrm{d}T_{\mathrm{After\_reaction}} - \sum_{\mathrm{i}} n_{i,\mathrm{in}} \int_{298}^{\mathrm{Tin}} C_{p,i}\mathrm{d}T_{\mathrm{Before\_reactions}} \quad (7)$$

$$Q_{\mathrm{Oxidant}} = n_{\mathrm{out}} \int_{298}^{\mathrm{Tout}} C_{p,i}\mathrm{d}T - n_{\mathrm{in}} \int_{298}^{\mathrm{Tin}} C_{p,i}\mathrm{d}T \quad (8)$$

$$Q_{\mathrm{radiation}} = f_{12} A_s \sigma (T^4_{\mathrm{Stack\_Surface}} - T^4_{\mathrm{Enclosure}}) \quad (9)$$

The view factor, f_{12}, can be calculated from stack geometry and materials properties [13], and it was approximated as 1.0 in this design assuming complete enclosure of the stack. Assuming that the stack is in a small enclosure filled with air, there will also be natural convection from the stack surface, where

$$Q_{\mathrm{Convection}} = h A_S (T_{\mathrm{Stack\_Surface}} - T_{\mathrm{Enclosure}}) \quad (10)$$

Using the dimensionless Prandtl (N_{pr}), Grashof (N_{Gr}) and Nusselt (N_{Nu}) numbers: when $N_{\mathrm{pr}}N_{\mathrm{Gr,d}} < 2 \times 10^3$, $N_{\mathrm{Nu,d}} = hd/k = 1.0$ [14]. For $d = 0.01$ m in air,

$$h = \frac{k}{\delta} \approx 6.75 \frac{W}{m^2\,\mathrm{K}} \quad (11)$$

where d is the gap thickness between the stack surface and enclosure. This thermal management analysis is based on assumptions of stack surface and enclosure temperatures, which are modeled here as constants. In practice, a variable temperature profile will exist at these surfaces as well as within the stack; computer-aided finite element analysis can determine these profiles.

The stack surface temperature is dependent upon the operating current, cell size, and cell materials—all of these variables affect heat generation and the conduction through the stack and radiation/convection from the stack. Increasing the thermal conductivity of the stack (by increasing the thickness of the metallic interconnects, for example) will help to ensure adequate heat removal from the stack to minimize both the temperature gradients within the stack and the required oxidant flow rate. However, increasing the interconnect thickness will also make the stack larger and heavier as well as increase ohmic resistance. Ideally, the temperature drop between the center point of the stack and the hottest point should be no more than 100° to minimize thermal stresses, current instabilities, and area specific resistance, which is conservatively estimated to be 1.5 Ω-cm^2 [15,16].

3.2. Reformer thermal balance

Thermal management of the reformer is equally important. The energy balance would be the following during steady state operation:

$$Q_{\mathrm{ref,rxn}} + Q_{\mathrm{fuel,evap}} + Q_{\mathrm{ref,products,preheat}} + Q_{\mathrm{Burner,comb\_rxn}} + Q_{\mathrm{Shift,rxn}} + Q_{\mathrm{Steam\_recycle\_cooldown}} + Q'_{Stack} = 0 \quad (12)$$

where the first three terms are heat sinks and the last four are heat sources,

$$Q_{\mathrm{ref,rxn}} = \Delta_{\mathrm{rxn}} \mathrm{H}_{\mathrm{ref},\mathrm{C_{12}H_{26}}(g),298\,\mathrm{K}}(\dot{n}_{\mathrm{C_{12}H_{26}}}) \quad (13)$$

$$Q_{\mathrm{Burner,comb\_rxn}} = \Delta_{\mathrm{rxn}} \mathrm{H}_{\mathrm{H_2comb},298\,\mathrm{k}}(2\dot{n}_{\mathrm{O_2,inlet\_burner}}) \quad (14)$$

$$Q_{\mathrm{fuel,evap}} = \Delta_{\mathrm{vap}} \mathrm{H}_{\mathrm{C_{12}H_{26}},489\,\mathrm{K}}(\dot{n}_{\mathrm{C_{12}H_{26}}}) \quad (15)$$

$$Q_{\mathrm{Steam\_recyle\_cooldown}} = -\sum_i n_i \int_{298}^{\mathrm{Tin}} C_{p,i}\mathrm{d}T_{\mathrm{Before\_reactions}} \quad (16)$$

$$Q_{\mathrm{ref\_products\_preheat}} = -\sum_i n_i \int_{298}^{\mathrm{Tout}} C_{p,i}\mathrm{d}T_{\mathrm{After\_reactions}} \quad (17)$$

After solving for x in Eq. (5) at the outlet temperature,

$$Q_{\mathrm{Shift}}, \mathrm{rxn} = \Delta_{\mathrm{rxn}} \mathrm{H}_{\mathrm{Shift},298\,\mathrm{K}}(x) \quad (18)$$

In this reformer balance, it is important to distinguish between the steam line and the liquid hydrocarbon fuel inlets; each has a different inlet temperature and composition as indicated in Table 1. Combustion at the reformer burner is fueled by the exhaust gas from the stack after water has been condensed out of the stream. Q'_{Stack} refers to the amount of heat that needs to be transferred from the SOFC stack to the reforming process. Q'_{Stack} is solved by Eq. (12) after solving for all other terms.

4. Results

4.1. Compactness and weight limit

Fig. 1 shows the general process flow of the SOFC power system. Table 3 summarizes the estimated volume and mass

Table 3
Masses and volumes of system components[a]

Component	Mass (kg)	Volume (L)
300 cell SOFC stack (8 cm × 8 cm)	10	10
Insulation	4	5
Steam reformer/burner	5	2
Oxidant storage (LOX)	54	48
LOX Tank fabricated from aluminum and incorporated into UUV hull	<40	~50
Dodecane/JP-8 storage	18	23
Fuel tank	4	4
Steam recuperator/condensor	15	10
Pumps (5 total)	16	10
Recirculation fan	4	2
Bussing	5	5
Trim	To be determined	To be determined
BoP (piping, circuits, etc.)	5	5
Total	180	174

[a] Based on 3 kW stack (2.5 kW net output) for 40 h.

of each system component. These are optimal guidelines for developers. Ultimately, if a given element needs to be larger, then it will do so at the expense of diminishing the fuel and oxidant supplies along with the lifetime of the mission. The most significant element is the LOX storage tank, which comprises over half the available volume. In order to fit enough oxygen in the system, the LOX tank will have to be merged with the UUV hull. Because the UUV chamber temperature will likely be elevated, hull incorporation may afford the LOX tank added protection against temperature rise. The condenser/heat exchanger attributes will most likely not be met with standard tube-in-tube designs. Wicking, desuperheaters, or micro-channeled heat exchangers will probably be required to meet these mass and volume metrics. Based on the values given in Table 3, there is potential for this system to fit within the volumetric and mass requirements. There may also be additional room left for trim and other balance of plant components.

4.2. Thermal balances

The most critical thermal balances of the system surround the SOFC stack and the steam reformer. Based on the energy balance in Eq. (3)–(10), Table 4 shows the heat flows calculated for two 150 cell stacks with the following assumptions.

Average enclosure $T = 1100$ K; average stack surface $T = 1110$ K; number of cells, $N = 300$; total surface area of stacks, $A_s = 0.45$ m^2; feed of pure dodecane at 9.535 mL min^{-1} (0.042 mol min^{-1}); steam/carbon ratio = 3.00; stack current, $I = 12.8$ A; voltage per cell, $V_{\text{operating, cell}} = 0.8$ V; active area of each cell = 64 cm^2; individual cell open circuit voltage = 1.1 V; area specific resistance of SOFC stack = 1.5 Ω-cm^2; fuel gas inlet composition (molar): 48.7% H_2, 31.6% H_2O, 7.8% CO_2, 11.9% CO; fuel gas inlet $T = 1055$ K; fuel gas outlet composition (molar): 10.7% H_2, 69.6% H_2O, 16.3% CO_2, 3.3% CO; fuel gas outlet $T = 1130$ K; fuel gas flow rate (in = out) = 2.56 mol min^{-1}; oxidant inlet composition: 100% O_2; oxidant inlet $T = 1040$ K; oxidant outlet composition: 100% O_2; oxidant outlet $T = 1130$ K; oxidant flow rate in = 11.21 mol min^{-1}; oxidant flow rate out = 10.61 mol min^{-1}.

With a thermal neutral voltage of 1.29 V (based on the lower heating value of hydrogen), the heat generated from the stack is:

$$(1.29\,\text{V} - 0.8\,\text{V})(0.2\,\text{A cm}^{-2} \times 64\,\text{cm}^2) \times 300\,\text{cells} = 1883\,\text{W}$$

in addition to 123 W from the water–gas shift reaction. Assuming that 70% of this heat dissipates from the stack surfaces and that the maximum temperature change of the fuel stream is 75°,

Table 4
Steady state SOFC stack energy balance

Heat sourIces	W	HeatI sinks	W
Q_{Stack}	1883	Q_{FuelGas}	−282
$Q_{\text{Shift, rxn}}$	123	Q_{Oxidant}	−320
		$Q_{\text{Radiation}}$	−1378
		$Q_{\text{Convection}}$	−26
Total	2006		−2006

Table 5
Steady state reformer energy balance

Heat sources	W	Heat sinks	W
$Q_{\text{Burner,comb\_rxn}}$	715	$Q_{\text{ref,rxn}}$	−1311
$Q_{\text{Shift,rxn}}$	137	$Q_{\text{fuel,evap}}$	−43
$Q_{\text{Steam\_recycle\_cooldown}}$	773	$Q_{\text{ref,products,preheat}}$	−1088
Q'_{Stack}	817		
Total	2442		−2442

320 W must be removed by the oxidant stream. Given that? $T_{O_2} = T_{\text{outlet},O_2} - T_{\text{inlet},O_2}$ is 90° (857–767 °C), the inlet flow rate of oxygen needs to be 11.21 mol min^{-1} to provide adequate cooling to the SOFC stack.

The various heat flows around the reformer are summarized in Table 5, and it is assumed that steam is recycled at 767 °C (1110 K) back into the reformer to react with 298 K dodecane. Thermal balances around the fuel cell and reformer have been conducted to effectively manage heat dissipation into the UUV chamber. Table 6 lists the heat sources and sinks present in this system with expected values of heat generation or absorption. While the calculations use heat of reaction values at 25 °C (298 K), the "anticipated temperature range" columns list the expected temperature range in which each process/reaction will take place. Table 6 is separated into four divisions to show which sources and sinks should be coupled for heat exchange. Heat dissipated by parasitic devices and electronics must also be accounted for in the total energy balance.

5. Discussion

5.1. UUV thermal management

The key aspect of this system is the use of waste heat from the SOFC stack to drive the reforming reaction to completion and provide the final preheat of the gas to the proper inlet temperature for the SOFC stack. To reach maximum system efficiency, roughly 60% of the heat dissipating from the SOFC stack surfaces must be used for the fuel reforming process. The best method of doing this is still uncertain, but it might be accomplished by splitting the reformer into two stages. The initial reforming step (heated by the fuel exhaust and burner) converts dodecane to a methane-rich reformate. The secondary reformer uses the stack radiant and convective heat to complete full reformation to a H_2-rich gas preheated to 782 °C (1055 K). Because this split reformer has yet to be demonstrated, Stream 3 in Table 1 is still under investigation. The state of Stream 3 will depend on how efficient heat transfer is from the SOFC stack to the secondary reformer via radiation and convection. Another design would be to couple the regenerative steam heating loop with the radiative heat from the SOFC stack. This would transfer heat from the SOFC stack to steam that is used in the steam reformer.

5.2. UUV performance (net power output)

Estimates of the power requirements for other parasitic devices are shown in Table 7, and when these losses are

Table 6
Overall heat balance of UUV energy section

Source (with temperatures used in calculation)	Anticipated T range (K)	W	Sink (with temperatures used in calculation)	Anticipated T range, K	W
Division 1					
Steam recycle cooldown(1110-298 K)	1110–500	773	Dodecane evaporation @298 K	489	43
Burner for reformer	∼850–950	715	Reforming reaction of dodecane @298 K	500–1055	1311
Fuel cell stack heat generation	1130	1883	Fuel gas preheat before entering Stack (298–1055 K)	298–1055	1088
Shift reaction @ 298 K (in reformer and fuel cell)	500–1130	137 + 123	Fuel gas in stack (1055–1130 K)	1055–1130	282
			Oxidant gas in stack (1040–1130 K)	1040–1130	320
			Excess heat from stack to UUV chamber	373–1000	587
Division 2					
Oxidant cooldown (1130 to 1040 K)	1130–1040	560	LOX heat up from 298 K–1040 K	298–1040	240
			Heat transfer to seawater	298–1130	320
Division 3					
Excess heat from stack	∼900	587	Condensed H_2O conduction to sea	350–363	587
Division 4					
			LOX heat up to 298 K	123–298	60
Devices (pumps, fans, electronics, etc.)	UUV chamber T, (∼323)	500	Dissipation through UUV hull to sea (293 K)	323	440

subtracted from the total power output of the SOFC stacks, the net power out is 2.5 kW with overall system efficiency of approximately 45%, based on the lower heating value of the dodecane. Major parasitic losses are expected to be the control system and oxidant recirculation fan, which is required to conserve the oxygen supply. The SOFC stack will have to run at roughly 3 atm inlet gas pressure and 2.8 atm outlet to have the 60%-efficient oxidant fan's load be near 200 W. While 1 atm was used in the other calculations, pressurization is likely for the final design and can potentially increase SOFC and system efficiencies barring gas leakage at stack seals.

Two 150-cell, SOFC stacks will enable 25.6 A at the 2.5 kW maximum continuous power output. The stacks can run at higher power, but this would decrease the stack efficiency and generate more heat, which could lead to system overheating. To maintain high efficiency and prevent overheating the system, the SOFC stack should be operated below its maximum power density. The amount of waste heat from the stack is proportional to the area specific resistance of the stack. Lower resistance will enable higher stack efficiency, which should translate into a greater feasibility for this system. The value of 1.5 Ω-cm^2 was taken as a conservative estimate of current stack technology, but this value could be much lower as SOFC stack technology matures.

Table 7
Balance of plant, net power output

Component	Power (W)
SOFC stacks total power output	3072
Oxidant fan for recirculation	−200
Steam injector	−50
Fuel pump	−50
Excess gas pump overboard	−100 (periodic)
Oxygen fan to burner	−50
Control system	−100
Valves (6)	−5
Net power output	∼2500
Overall system efficiency[a] (%)	∼45

[a] Based on LHV of dodecane fed into system.

5.3. Product disposal

An effective means of recycling the steam product from the fuel cell while disposing of the CO_2 is of paramount importance to the successful system design. CO_2 accumulation will lower stack efficiency, increase flow rates and pressure in the system, and may ultimately lead to carbon deposition. After condensing out the water needed for the reformer, the gaseous products and extra water will be stored under pressure until the pressure is high enough to pump them overboard. Periodic purging of the gas overboard activated by a pressure sensor will prevent over-pressurizing the system. The gas mixture will consist primarily of H_2, H_2O, CO, and CO_2 and will have minimal impact on the seawater environment, especially considering the scale of the vehicle. To counter the loss in mass, seawater would flow into the UUV to maintain proper buoyancy.

6. Conclusions

A system-level analysis of an energy section for a SOFC-powered 21″ UUV has been presented. Component size and mass have been targeted, and the energy balance around each

component has been modeled in order to address the thermal management this system requires to achieve maximum efficiency. Volume is the most stringent constraint, and mission lifetime will depend highly upon the amount of oxidant that can be stored. A system efficiency that approaches 45% based on the lower heating value of the hydrocarbon fuel is the initial goal and will depend on careful system integration of the SOFC stack, fuel reformer, fuel/oxidant storage and balance of plant components. A pivotal step towards final assembly will be validating a coupled SOFC stack/steam reformer that utilizes the waste heat and water from the SOFC stack in the steam reforming process.

In spite of these hurdles, SOFC technology offers a UUV power system that may achieve the Navy's targeted goal, which is a refuelable UUV power source comparable in performance to state-of-the-art primary batteries. An energy density of 400–600 W h kg^{-1} and specific energy of 400–600 W h L^{-1} appear to be feasible. With careful management of the LOX system, the safety level of a hydrocarbon-fueled SOFC system should be favorable to a primary lithium battery, which must be stored and transported in a fully charged state. Capital costs and reliability are still the major drawbacks to SOFC technology, but continued development by industry will make them economically competitive with battery technologies. Even a modest cycling capability (30–40 cycles) would offer large savings over primary batteries, which must have their entire energy section replaced after each mission.

Acknowledgements

The authors would like to thank the following people for technical discussion on specific aspects of this system: Joe Hartvigsen (Ceramatec) for sharing information on SOFC stack operation, Jeff Harrison (formerly of InnovaTek) for input on the steam reformer design, Adam Culler (Sierra Lobo) for discussions on LOX system storage. Mark Cervi (Naval Surface Warfare Center in Philadelphia, PA) for discussion on thermodynamic issues, and Chris Egan (Naval Underwater Warfare Center, Division Newport) for supplying the UUV power requirements.

References

[1] R.R. Bessette, M.G. Medeiros, C.J. Patrissi, C.M. Deschenes, C.N. LaFratta, J. Power Sources 96 (2001) 240–244.
[2] Q. Li, R. He, J. Gao, J.O. Jensen, N.J. Bjerrum, J. Electrochem. Soc. 150 (2003) A1599–A1605.
[3] S.C. Singhal, J. Mizusaki (Eds.), Proceedings of the International Symposium, Solid Oxide Fuel Cells IX, Quebec City, Que., Canada, May 2005, pp. 48–97.
[4] R.W. Sidwell, W.G. Coors, J. Power Sources 143 (2005) 166–172.
[5] Fuel Cell Handbook, seventh ed., by EG&G Technical Services, Inc., DOE sponsored contract No. DE-AM26-99FT40575, November 2004.
[6] U.S. Navy UUV Master Plan found at www.chinfo.naw.mil/navpalib/technology/uuvmp.pdf.
[7] P. Arkoudeas, S. Kalligeros, F. Zannikos, G. Anastopoulos, D. Karonis, D. Korres, E. Lois, Energy Convers. Manage. 44 (2003) 1013–1025.
[8] C. Obringer, USAF Fuels Program Overview, CRC Aviation Meeting, Wright-Patterson Air Force Base, 29 April–2 May 2002.
[9] Q. Ming, T. Healey, L. Allen, P. Irving, Catal. Today 77 (2002) 51–64.
[10] A.C. Khandkar and S. Elangovan, United States Patent 5,763,114, June 9 1998, Gas Research Institute.
[11] D.L. Damm, A.G. Federov, J. Power Sources 143 (2005) 158–165.
[12] P. Li, K. Suzuki, J. Electrochem. Soc. 151 (2004) A548–A557.
[13] V.R. Rao, V.M.K. Sastiri, Int. J. Heat Mass Transfer 39 (1996) 1281–1286.
[14] C.J. Geankoplis, Transport Processes and Unit Operations, second ed., Allyn and Bacon, Newton, MA, 1983, pp. 244–250.
[15] H. Yakabe, T. Ogiwara, M. Hishinuma, I. Yasuda, J. Power Sources 102 (2001) 144–154.
[16] M. Mangolda, M. Krasnyka, K. Sundmacher, Chem. Eng. Sci. 59 (2004) 4869–4877.